Supplementary Information.

Supplemental Figures.

Figure S1

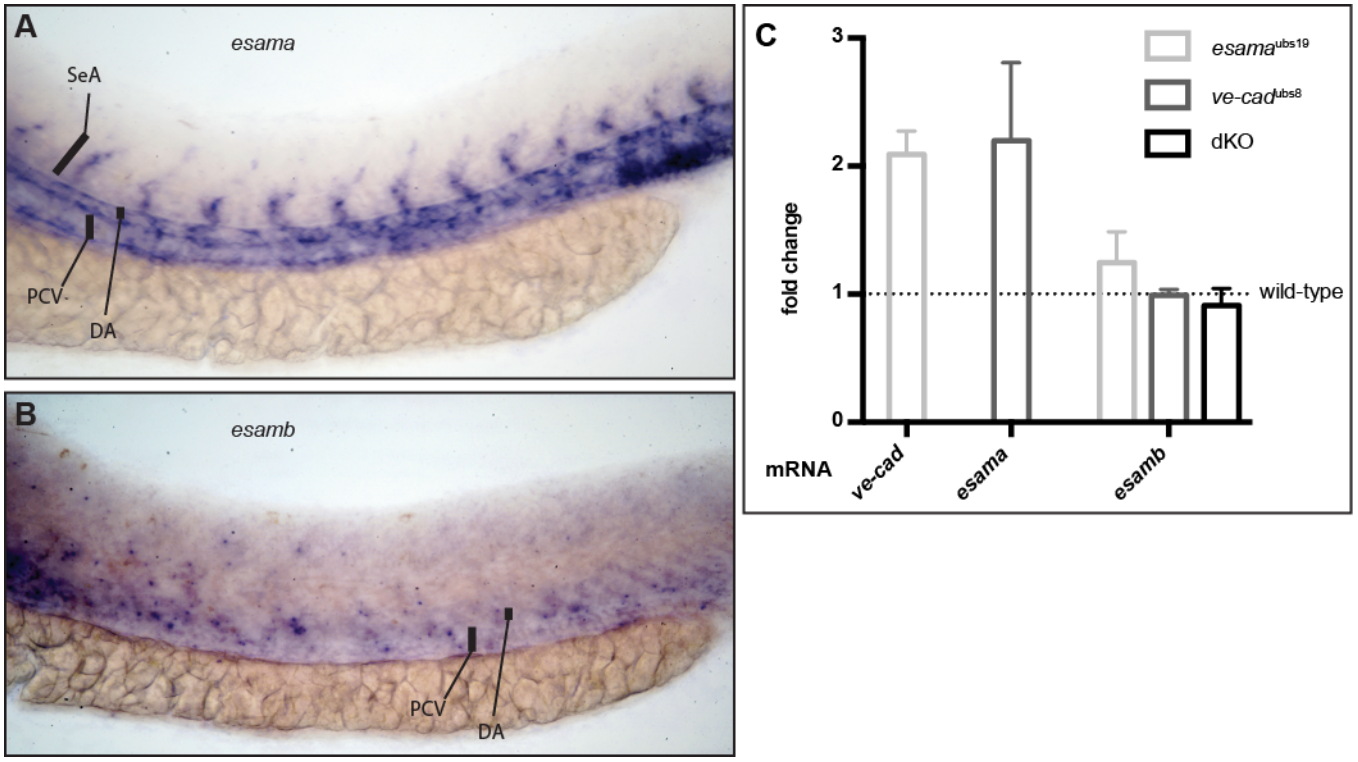

Figure S1: Esama is specifically expressed in the trunk vasculature

In situ hybridization for *esama* (A) and its paralog *esamb* (B) expression in embryos at 28 hpf. (**A**) *esama* is expressed in the DA, PCV and the growing SeAs. (**B**) *esamb* expression appears to be very weak in the trunk vasculature. The colorimetric reaction was prolonged, but stopped to prevent too strong background. DA, dorsal aorta; SeA, segmental artery; PCV, posterior cardinal vein. (**C**) Quantitative RT-PCR analysis of *ve-cad, esama* and *esamb* transcripts in different mutant genotypes. mRNA levels are compared relative to wild-type embryos. Experiments were performed in 3 biological and 3 technical replicates. dKO, double mutant.

Figure S2

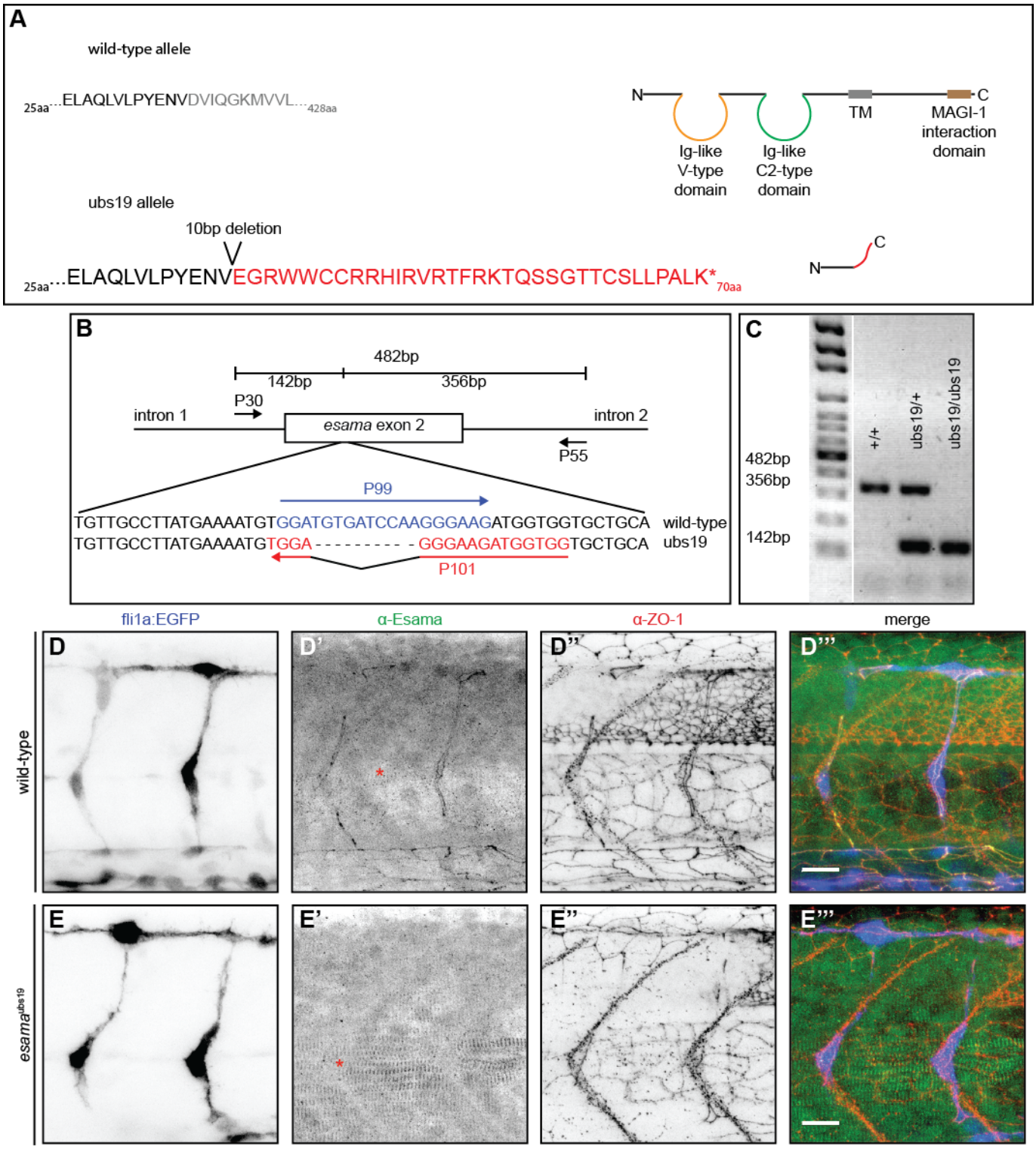

Figure S2: Generation and verification of an *esama* mutant allele

(**A**) Schematic representation of the wild-type and *esama*^{ubs19} mutant allele. Top: the amino acid sequence of wild-type Esama (total of 428aa) flanking the region of mutagenesis and schematic drawing of wild-type Esama. Esama harbors two N-terminal extracellular Ig-like domains (one V- and one C2-type), a single transmembrane domain and a long cytoplasmic tail harboring a MAGI-1 binding domain. Bottom: the 10bp deletion leads to a frame shift, which alters Esama's sequence

after the first 37aa and leads to a premature stop after a total of 70aa (altered amino acid sequence highlighted in red). This premature stop leaves only a very short peptide.

(**B** and **C**) Genotyping PCR strategy (B) and examples of amplicons produced by wild-type, *esama*^{ubs19} heterozygous or homozygous mutants. (A) The external primers (P30 and P55) flank exon 2 and amplify both, mutant and wild-type alleles (482bp). This amplicon is outcompeted by the smaller wild-type and ubs19 products. P99 specifically anneals to the wild-type sequence and produces a band of 356bp with P55. P101 is specific for the mutation and together with P30 generates a 142bp product.

(**D** and **E**) Confocal images of wild-type (D) and *esama*^{ubs19} (E) Tg(*fli1a:EGFP*)^{y1} (blue) embryos stained for Esama (green) and Zo-1 (red), single channels are shown in inversed contrast, anterior to the left. The architecture of SeAs looks similar between wild-type and *esama*^{ubs19} (compare the EGFP channels D and E); there are no obvious angiogenic defects in the mutant. The staining for Esama confirms the loss of protein in the mutant background (E'). Importantly, the Esama antibody recognizes epitopes in the cytosolic C-terminal portion of the protein (Sauteur et al., 2014), excluding the possibility of splice variants in the *esama*^{ubs19} mutant background. The Esama antibody shows cross-reactivity with the myotome, which remains visible in the mutant (demarcated by red asterisks in D' and E'). aa, amino acid; TM, transmembrane domain, scale bars, 20µm.

Figure S3

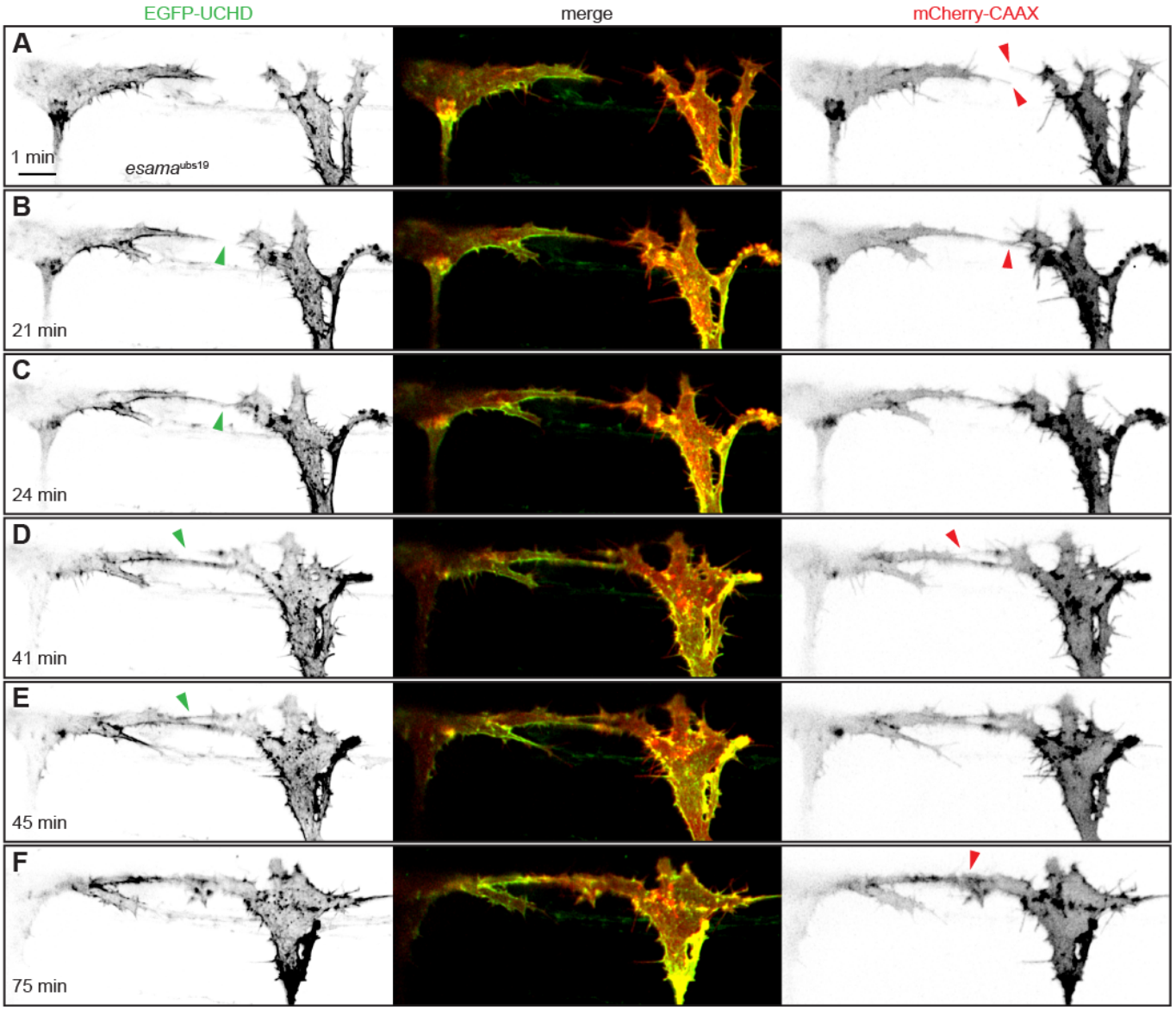

Figure S3: Loss of Esama does not lead to defects in anastomosis

(**A-F**) Still images from Movie S3 of an *esama*^{ubs19} mutant Tg(*fli1ep:gal4ff*)^{ubs3}, Tg(*UAS:EGFP-UCHD*)^{ubs18}, Tg(*kdrl:mCherry-CAAX*)^{s916} embryo at around 32hpf, anterior to the left. Single channels are shown in inversed contrast (green is EGFP-UCHD and red is mCherry-CAAX on left and right, respectively) and the merge is shown in the middle. (**A**) Two tip cells are extending filopodia (red arrowheads) towards each other. (**B**) A filopodial contact is established (red arrowhead), but actin cytoskeleton (green arrowhead) has not accumulated at the cell-cell bridge yet. (**C**) The cell-cell bridge is quickly stabilized with actin cytoskeleton (green arrowhead). (**D** and **E**) A second protrusion is established between the two tip cells (red arrowhead) and quickly stabilized with actin cytoskeleton (compare green arrowheads in C and D). (**F**) During contact maturation, the two cell-cell contact sites are fused to a single one (red arrowhead). Scale bar, 10µm.

Figure S4

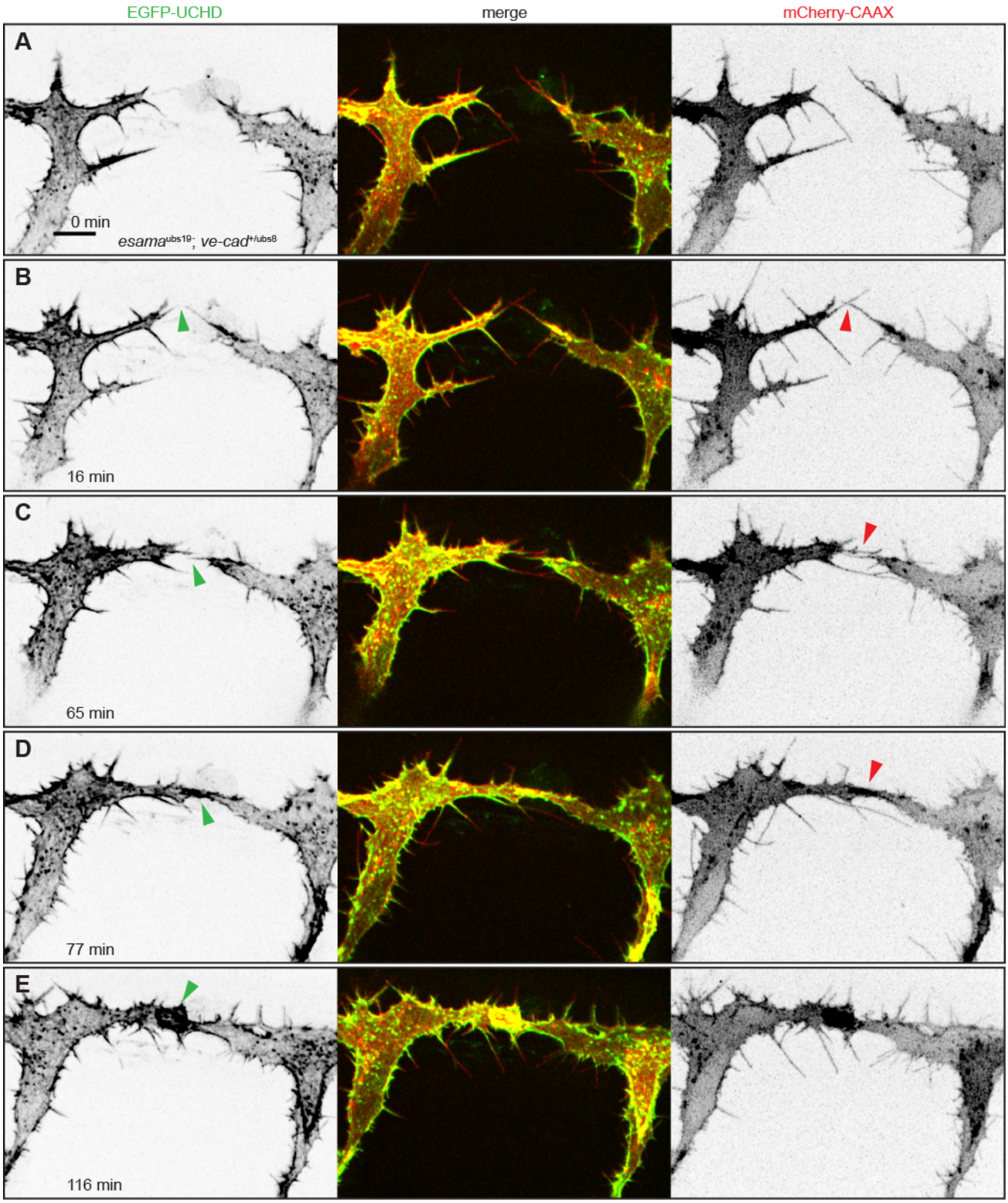

Figure S4: *esama*$^{-/-}$; *ve-cad*$^{+/-}$ embryos display an intermediate filopodial phenotype.

(**A-F**) Still images from Movie S9 of an *esama*^{ubs19}; *ve-cad*$^{+/ubs8}$ embryo. Tg(*fli1ep:gal4ff*)^{ubs3}, Tg(*UAS:EGFP-UCHD*)^{ubs18}, Tg(*kdrl:mCherry-CAAX*)^{s916} embryo at around 32hpf, anterior to the left. Single channels are shown in inversed contrast (green is EGFP-UCHD and red is mCherry-CAAX on left and right, respectively) and the merge is shown in the middle. (**A**) Two tip cells are extending filopodia towards each other. (**B**) Two filopodia touch (red arrowhead). (**C**) A filopodial contact is

established (red arrowhead) and actin cytoskeleton (green arrowhead) is being recruited to the cell-cell contact site. (**D**) The cell-cell bridge (red arrowhead) is quickly stabilized with actin cytoskeleton (green arrowhead). (**E**) Anastomosis led to the formation of a junctional ring between the two tip cells (green arrowhead). Scale bar, 10μm.

Figure S5

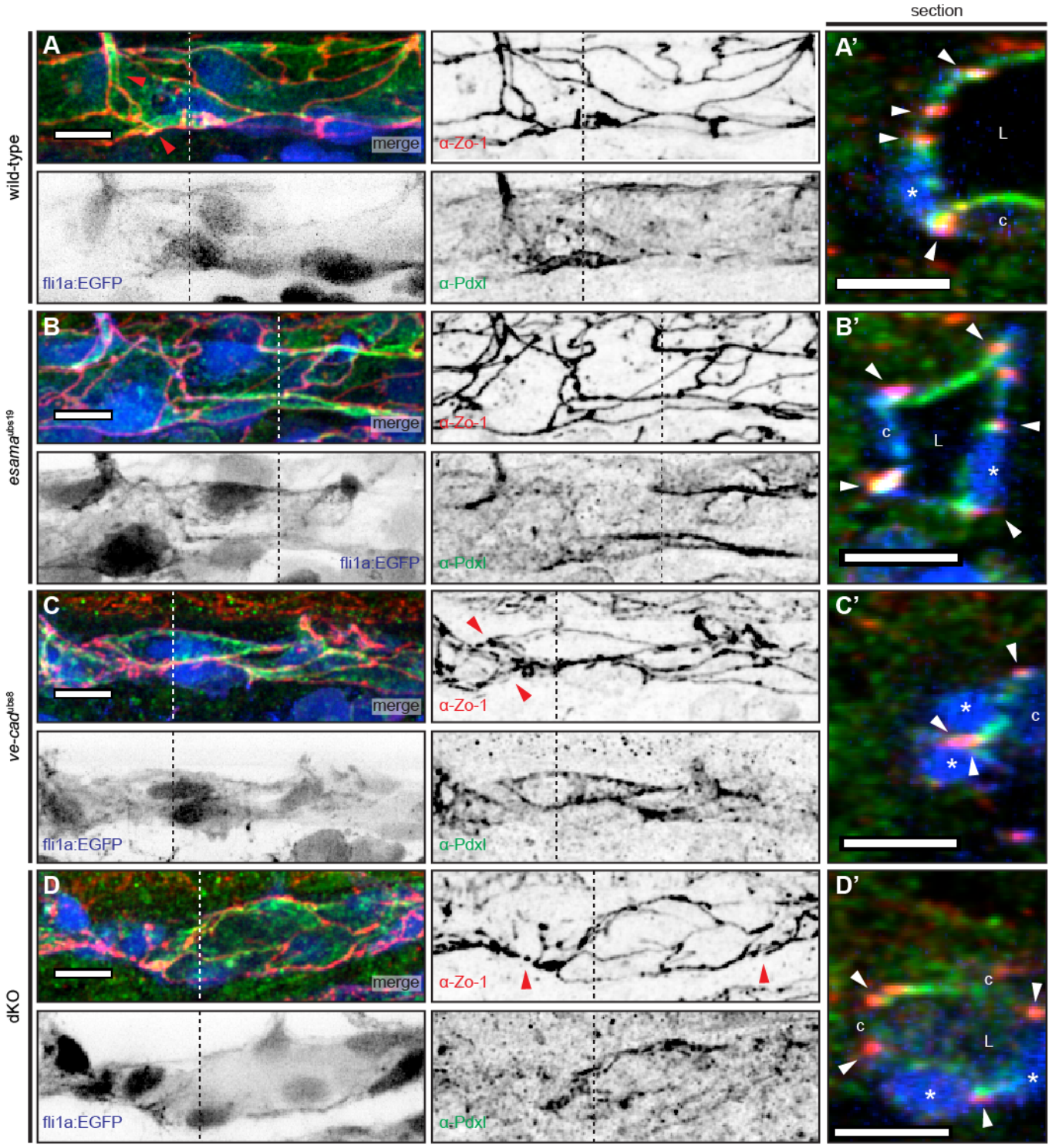

Figure S5: The DA appears to form normally in the absence of VE-cad and Esama

(**A-D**) Deconvolved projections of DAs of Tg(*fli1a:EGFP*)^{y1} (blue) wt (A), *esama*^{ubs19} (B), *ve-cad*^{ubs8} (C) and *esama*^{ubs19}; *ve-cad*^{ubs8} double mutant (dKO, D) embryos stained for Zo-1 (red) and Pdxl (green), around 32hpf. Single channels are shown in inversed contrast. (**A**) In wild-type embryos the DA is lumenized and the strongest signal for apical Pdxl is usually observed close to junctions (Zo-1, and see red arrowheads in A). (A') shows a cross-section through the DA. Several ECs surround the lumen (L); apical staining (green) is seen between junctions (arrowheads) and on the luminal side of ECs. (**B**) The DA in *esama*^{ubs19} mutant embryos forms similar to wild-type ones. (B')

shows lumen (L) surrounded by several cells and also here the apical Pdxl is located between junctions (arrowheads) and on the luminal side of cells. (**C**) In the absence of VE-cad, the DA is lumenized only partially. Cell-cell junctions look more disorganized compared to wild-type siblings (red arrowheads in the Zo-1 panel). (C') But even in collapsed portions of the DA, apical signal (green) is observed between junctions, where lumen would be expected. Section was chosen where three cells (two nuclei and one cell body form the DA; only two junctions are observed (red arrowheads), because two junctions overlap between the two cell nuclei (n). (**D**) Similar to *ve-cad*^{ubs8} mutants, the DA of dKO embryos is only partially inflated and the junctions appear disorganized (red arrowheads in the Zo-1 panel). (D') However, apical polarization appears normal with signal (green) between junctions and on the luminal (L) side of the endothelial cells. Section shows lumenized portion of the DA surrounded by 4 cells. DA, dorsal aorta; L, lumen; asterisk, nucleus; c, cell body; white arrowheads, junctions; Pdxl, Podocalyxin; cross-section is located at the dotted line; scale bars, 10µm.

Figure S6

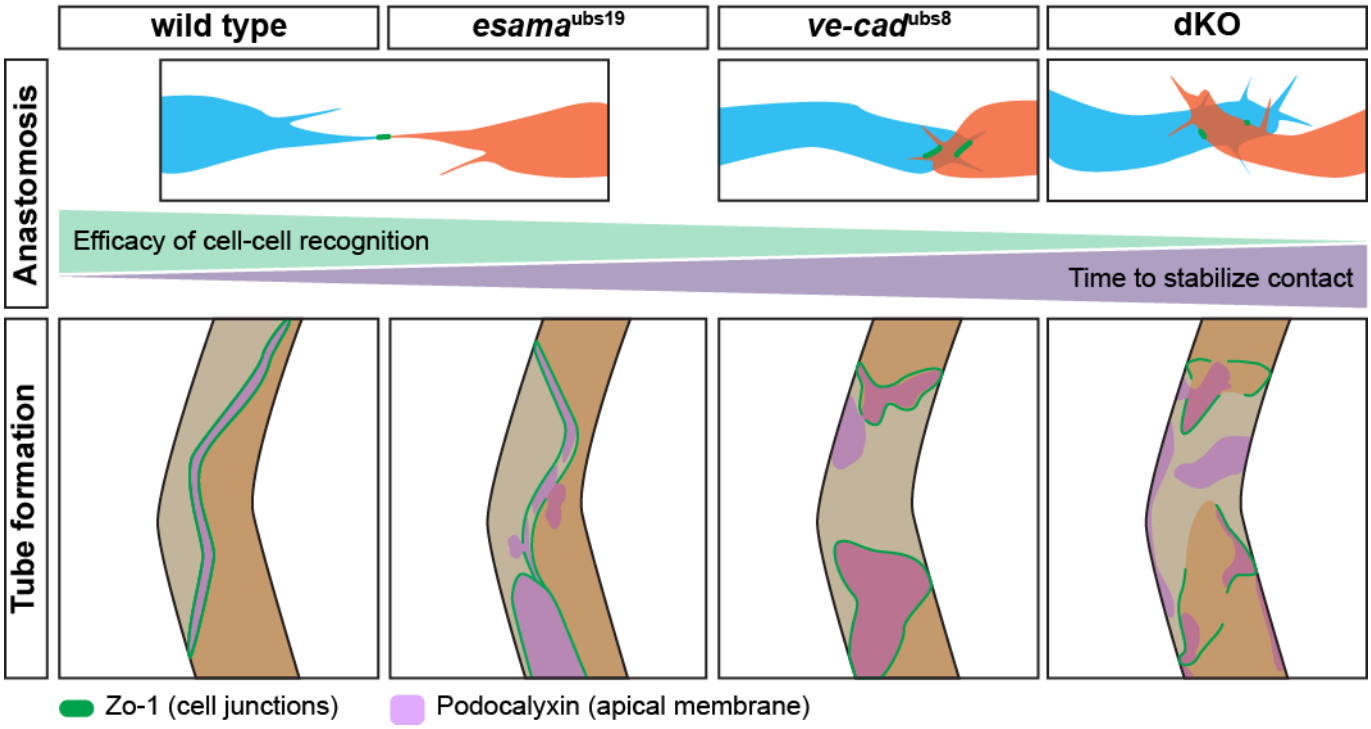

Figure S6: Schematic summary of *ve-cad* and *esama* mutant phenotypes

Top: tip cell interaction during anastomosis. In wild-type and *esama* mutants cell contacts are generated by filopodial contacts. In *ve-cad* mutants filopodial contacts are inefficient and contacts are established by endothelial cell bodies. In *esama*; *ve-cad* mutant embryos (dKOs), cell contact formation by filopodia, as well as cell bodies is basically inhibited.

Bottom: junctional dynamics during tube formation. During angiogenic sprouting of SeAs, wild-type junctions stretch over the whole SeA and apical Podocalyxin (Pdxl) is contained within the junctional ring. *esama* mutants show small gaps in their junctions (based on Zo-1 distribution), which correlates with mislocalized Pdxl (outside of the junctional ring). *ve-cad* mutants stalk cells show reduced cell rearrangement and elongation, and junctions occasionally show small gaps (smaller compared to *esama* mutants). dKO show an enhanced phenotype with reduced cell-cell adhesion, accompanied by enlarged gaps of Zo-1 at cell junctions. The size of junctional gaps correlates with the mislocalization of Pdxl.

Supplemental Table 1: qPCR primer list

Primer name	Sequence (5'->3')
RPS11-fwd	ACAGAAATGCCCCTTCACTG
RPS11-rev	GCCTCTTCTCAAAACGGTTG
beta-actin-fwd	CCACGAGACCACCTTCAACT
beta-actin-rev	CTTCTGCATCCTGTCAGCAA
esama-fwd	CAGCACAAAACCAAGCCG
esama-rev	GCTTATCAATTCCAGTCCGTTC
esamb-fwd	GCTTCGCCTCAATGTCAAAG
esamb-rev	TGCCATAGCCCGATTTACAG
ve-cad-fwd	CAGTGGGTCTAACCTGGATTATG
ve-cad-rev	AACCACAGTCTCCATCAAGC

Supplemental movies.

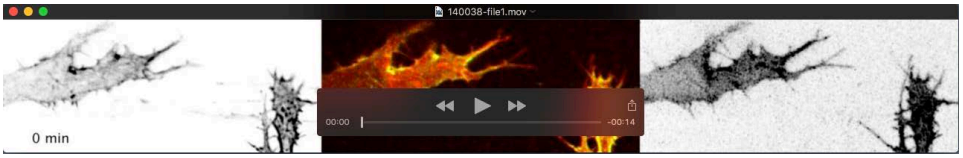

Movie 1: Anastomosis in a wild-type embryo

Deconvolved spinning disc confocal movie of a Tg(*fli1ep:gal4ff*)^{ubs3}, Tg(*UAS:EGFP-UCHD*)^{ubs18}, Tg(*kdrl:mCherry-CAAX*)^{s916} embryo at around 32hpf, anterior to the left. Confocal stacks were acquired every minute. Single channels are shown in inversed contrast (green is EGFP-UCHD and red is mCherry-CAAX on left and right, respectively) and the merged channels are shown in the middle. Two tip cells expand filopodia towards each other. Few transient filopodial interactions are observed before a single filopodial contact is maintained and reinforced by the recruitment of actin cytoskeletal components (around the 84th minute of the movie). The cell-cell contact matures and the actin cytoskeleton reorganizes to form junctional ring between the two tip cells (around 129th minute of the movie).

Movie 2: Anastomosis in a VE-cad morphant embryo

Deconvolved spinning disc confocal movie of a Tg(*fli1ep:gal4ff*)^{ubs3}, Tg(*UAS:EGFP-UCHD*)^{ubs18}, Tg(*kdrl:mCherry-CAAX*)^{s916} embryo injected with VE-cad morpholino. Movie was recorded around 32hpf, anterior to the left. Confocal stacks were acquired every minute. Single channels are shown in inversed contrast (green is EGFP-UCHD and red is mCherry-CAAX on left and right, respectively) and the merged channels are shown in the middle. Two tip cells extend filopodia towards each other. Many transient filopodial interactions are observed as the cell bodies of the two tip cells get closer to each other. Around the 89th minute, the tip cell on the right hand side establishes contact to the left one over two filopodia simultaneously. These two filopodia appear to be maintained and at the 92nd minute the two cell bodies touch. As the cell-cell contact expands junctions start to form between the two cells (seen in the EGFP-UCHD channel around the 165th minute). Cell-cell contact formation appears less efficient compared to wild-type siblings, and moreover, takes generally longer.

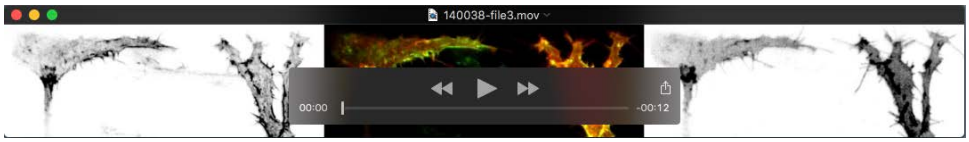

Movie 3: Anastomosis in an *esama*^{ubs19} mutant embryo

Deconvolved spinning disc confocal movie of a Tg(*fli1ep:gal4ff*)^{ubs3}, Tg(*UAS:EGFP-UCHD*)^{ubs18}, Tg(*kdrl:mCherry-CAAX*)^{s916} *esama*^{ubs19} mutant embryo at around 32hpf, anterior to the left. Confocal stacks were acquired every minute. Single channels are shown in inversed contrast (green is EGFP-UCHD and red is mCherry-CAAX on left and right, respectively) and the merged channels are shown in the middle. Similar to wild-type embryos, two tip cells expand filopodia towards each other. Few transient filopodial interactions are observed before a single filopodial contact is maintained and reinforced by the recruitment of actin cytoskeletal components (around the 24th minute of the movie). Shortly after, a second protrusion, made by the tip cell on the right hand side, establishes contact to the left tip cell. This second contact is quickly reinforced by actin cytoskeletal components (around the 45th minute of the movie). As anastomosis progresses, the two contacts are fused to a single one (around 75th minute of the movie). We also observe the establishment of two anastomotic contacts, which are then fused to a single one, in wild-type embryos. Therefore, anastomosis in the absence of Esama is comparable to wild-type.

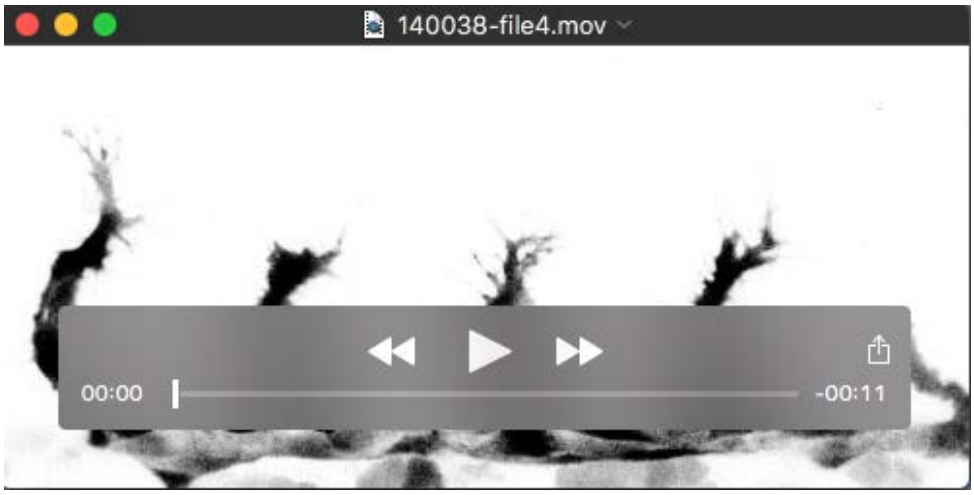

Movie 4: Angiogenesis in a wild-type embryo

Confocal movie of a Tg(*fli1a:EGFP*)^{y1} embryo starting around 26hpf (= 0min) shown in inversed contrast, anterior to the left. Confocal stacks were acquired every 10 minutes. The angiogenic sprouts expand dorsally and the first anastomotic contacts are observed around 31hpf (5h of the movie). As angiogenesis progresses lumen is pushed through the SAs into the DLAV (12h of the movie). At the end of the movie (~44hpf), all the SAs and the DLAV are lumenized.

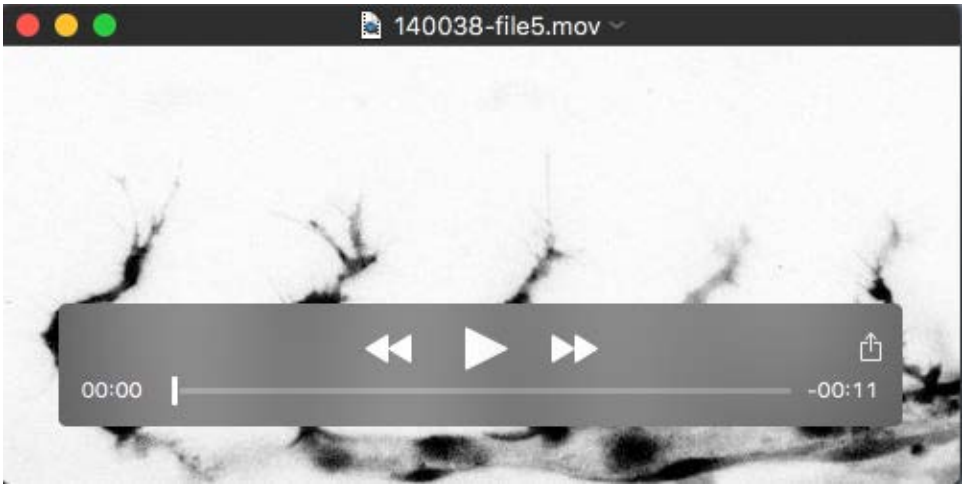

Movie 5: Angiogenesis in an *esama*^{ubs19} mutant embryo

Confocal movie of a Tg(*fli1a:EGFP*)^{y1} embryo starting around 26hpf (= 0min) shown in inversed contrast, anterior to the left. Confocal stacks were acquired every 10 minutes. Angiogenesis in *esama*^{ubs19} mutant embryo progresses indistinguishable from wild-type embryos. The angiogenic sprouts expand dorsally and the first anastomotic contacts are observed around 30hpf (4h of the movie). As angiogenesis progresses lumen is pushed through the SAs into the DLAV (12h of the movie). At the end of the movie (~44hpf), all the SAs and the DLAV are lumenized.

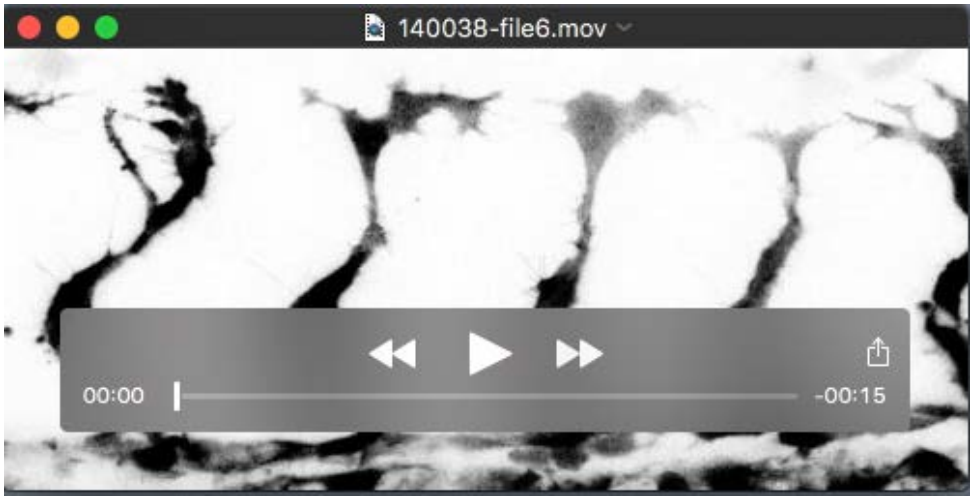

Movie 6: Angiogenesis in a *ve-cad*^{ubs8} mutant embryo

Confocal movie of a Tg(*fli1a:EGFP*)^{y1} embryo starting around 29hpf (26hpf = 0min) shown in inversed contrast, anterior to the left. Confocal stacks were acquired every 8 minutes. Tip cells of angiogenic sprouts start to anastomose around 30hpf (around 4h of the movie), which appears less efficient compared to wild-type embryos. In 34% of the SAs we observe detachments of tip cells from stalk cells, this examples however does not show this phenotype. Nevertheless, a basic vascular network, i.e. SAs and the DLAV, is formed. No lumen is pushed through the vessels due to the absence of blood pressure. However, sometimes lumen is observed in SAs up to the level of the horizontal myoseptum. The DA is mostly collapsed but may also show inflated portions.

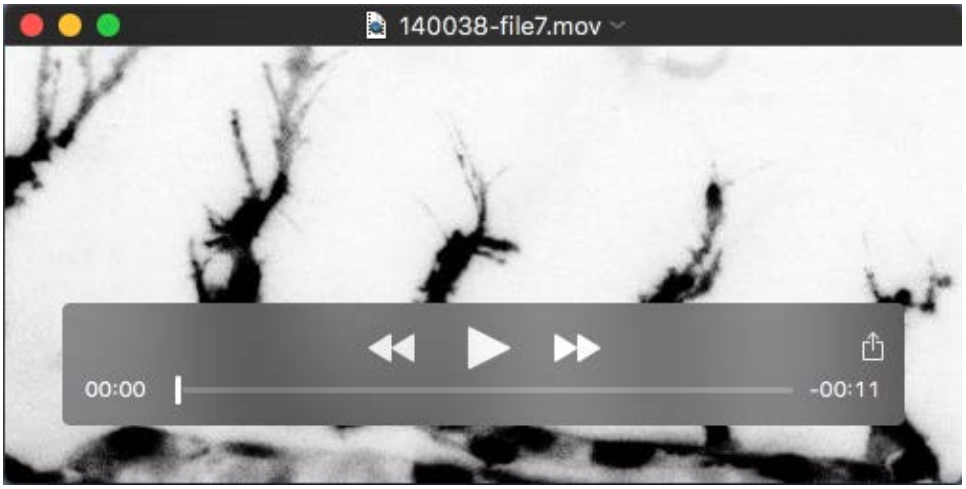

Movie 7: Angiogenesis in an *esama*^{ubs19}; *ve-cad*^{ubs8} double mutant embryo

Confocal movie of a Tg(*fli1a:EGFP*)^{y1} embryo starting around 29hpf (26hpf = 0min) shown in inversed contrast, anterior to the left. Confocal stacks were acquired every 8 minutes. Tip cells of angiogenic sprouts start to anastomose around 30hpf (around 4h of the movie), which is even less efficient compared to *ve-cad*^{ubs8} mutant embryos. In two SAs, the tip cells detach from the stalk (around 5h and 8h of the movie). The stalks of these two SAs do not manage to reattach to the tip cells in the DLAV within the time the embryo was imaged. This would be different in *ve-cad*^{ubs8} mutant embryos, where stalk cells that detached from their tip cell manage to reconnect to the DLAV within 8h after detachment. As angiogenesis progresses, cells in the DLAV appear not to integrate into a proper endothelium and retain their protrusive activity.

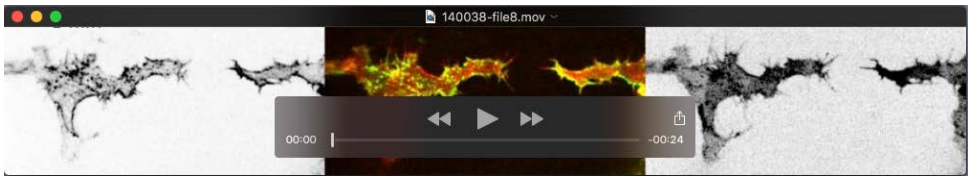

Movie 8: Anastomosis in an *esama*^{ubs19}; *ve-cad*^{ubs8} double mutant embryo

Deconvolved spinning disc confocal movie of a Tg(*fli1ep:gal4ff*)^{ubs3}, Tg(*UAS:EGFP-UCHD*)^{ubs18}, Tg(*kdrl:mCherry-CAAX*)^{s916} *esama*^{ubs19}; *ve-cad*^{ubs8} double mutant embryo at around 32hpf, anterior to the left. Confocal stacks were acquired every minute. Single channels are shown in inversed contrast (green is EGFP-UCHD and red is mCherry-CAAX on left and right, respectively) and the merged channels are shown in the middle. As the two tip cells migrate towards each other, they probe the environment for neighboring tip cells. Filopodia of the adjacent tip cells touch occasionally. At the 59th minute we observe a filopodial contact between the two tip cells, which appears to be reinforced by the actin cytoskeleton, but is resolved shortly after. As the two cell bodies get closer to each other, they start to touch and retract again. This happens several times and even when the two cell bodies overlap extensively (see 97th minute), they resolve the contact made. Eventually, the two tip cells appear to form a cell-cell contact and to maintain it (around the 201st minute of the movie). We imaged this embryo over 3h and anastomosis takes significantly longer compared to wild-type and even *ve-cad*^{ubs8} mutant embryos. In the last 20 minutes of the movie, we observe junction-like patterns with the EGPF-UCHD marker. However, in many other instances, we observed that some tip cells remain isolated, even after they tried to establish contact to neighbors.

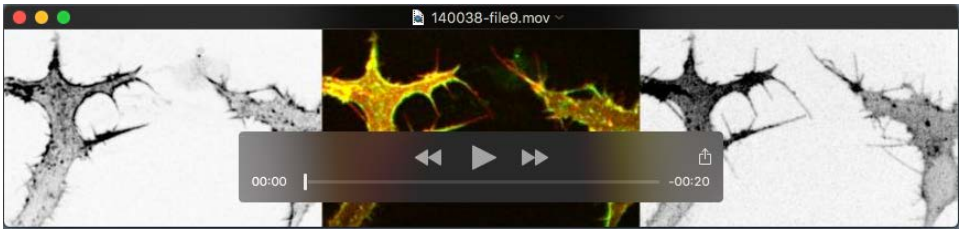

Movie 9: Anastomosis in an *esama*^{ubs19}; *ve-cad*$^{+/ubs8}$ mutant embryo

Deconvolved spinning disc confocal movie of a Tg(*fli1ep:gal4ff*)^{ubs3}, Tg(*UAS:EGFP-UCHD*)^{ubs18}, Tg(*kdrl:mCherry-CAAX*)^{s916} *esama*^{ubs19}; *ve-cad*$^{+/ubs8}$ mutant embryo at around 32hpf, anterior to the left. Confocal stacks were acquired every minute. Single channels are shown in inversed contrast (green is EGFP-UCHD and red is mCherry-CAAX on left and right, respectively) and the merged channels are shown in the middle. Similar to *ve-cad* mutant embryos, many transient filopodial interactions are observed. Only as the tip cell bodies are getting closer to each other and start to overlap (around the 66th minute) the filopodia/cell bodies do not retract and form an anastomotic contact.